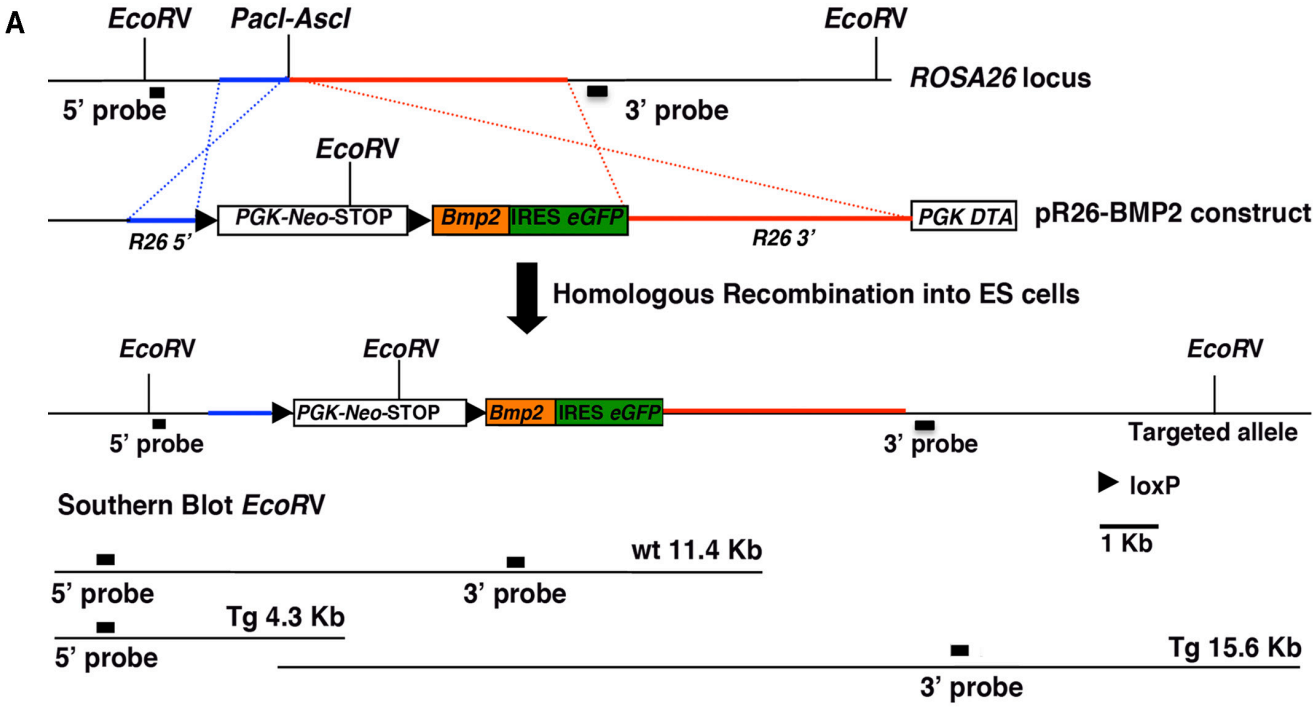

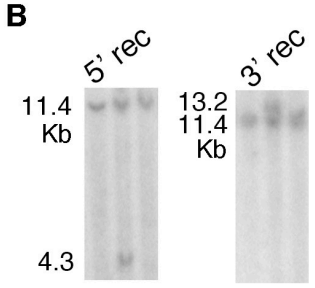

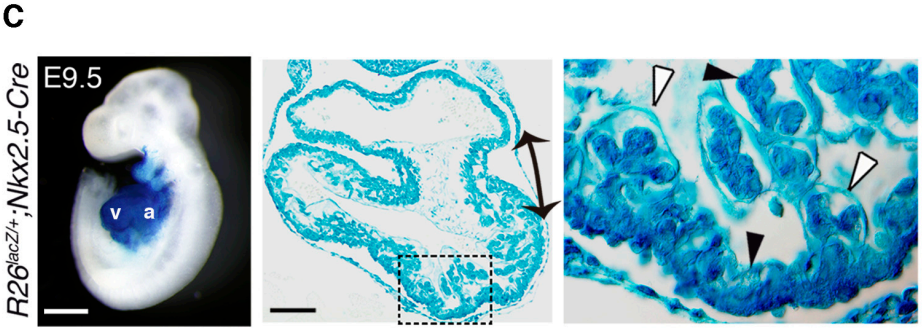

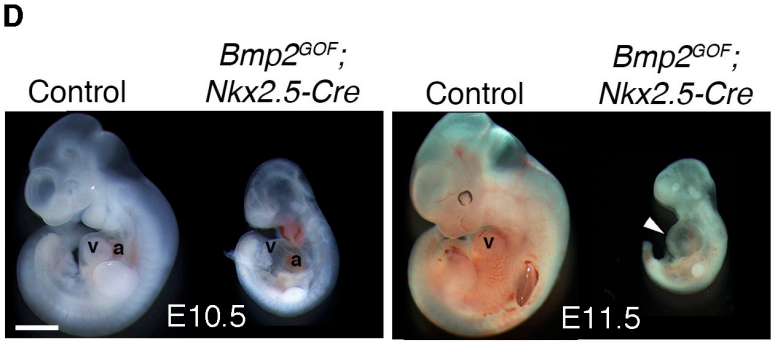

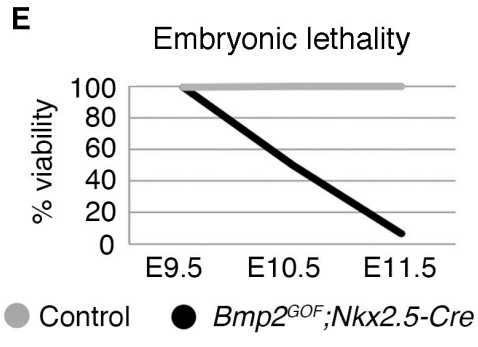

Fig. S1: Bmp2 overexpression causes early lethality in *Bmp2^{GOF};Nkx2.5-Cre* embryos

A) Gene targeting strategy for the generation of a conditional *Bmp2* transgenic line. The *Bmp2* transgene followed by *IRES-eGFP* was targeted into the *Rosa26* locus. **B)** Positive clones were identified by Southern blot using 5′ and 3′ arm probes and injected into C57/Bl6 blastocysts. **C)** Nkx2.5-Cre is active throughout the heart and in the pharyngeal arches, as shown with X-gal staining of *R26^{lacZ};Nkx2.5-Cre* embryos. The double arrows delimitate the AVC in the transverse section of the heart. Black arrowheads show myocardial and white arrowheads endocardial ventricular staining. **D)** At E10.5 and E11.5 *Bmp2^{GOF};Nkx2.5-Cre* embryos were underdeveloped and showed severe abnormalities. **E)** No significant mortality was observed at E9.5 transgenic embryos (n=136). Only 53% of transgenic embryos examined survived to E10.5 (n=15) and only 8% to E11.5 (n=13). Scale bars, 500µm (C, whole-mount), 100µm (C, sections), 1mm (D). v, ventricle; a, atrium.

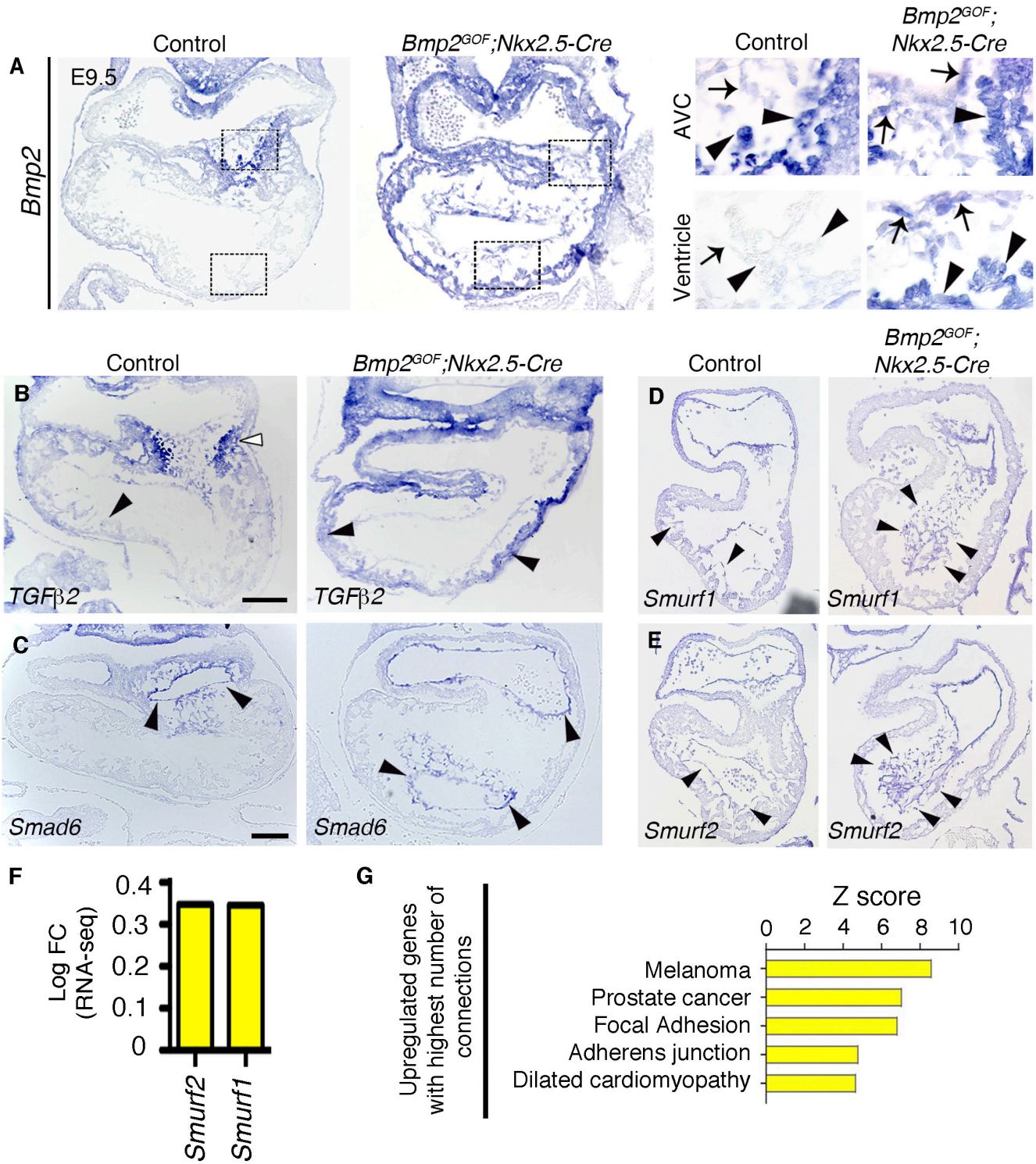

Fig. S2: *Bmp2* overexpression alters the transcriptional profile in *Bmp2^{GOF};Nkx2.5-Cre* hearts

A) The normal expression of *Bmp2* at E9.5 is restricted in AVC myocardium. No expression is seen in the endocardium (arrows) or in ventricular myocardium (arrowheads). Efficient activation of *Bmp2* in the myocardium (arrowheads) and endocardium (arrows) throughout the hearts of *Bmp2^{GOF};Nkx2.5-Cre* embryos. **B)** Expansion of *Tgfβ2* expression from the AVC (white arrowhead) to the whole myocardium (black arrowheads) in *Bmp2^{GOF};Nkx2.5-Cre* ventricles. **C)** The normally AVC restricted endocardial expression of *Smad6* at E9.5 was expanded to the chambers in *Bmp2^{GOF};Nkx2.5-Cre* hearts (arrowheads). **D)** *In situ* hybridisation of *Smurf1* showing increased expression in the endocardium of *Bmp2^{GOF};Nkx2.5-Cre* hearts at E9.5 (arrowheads). **E)** Increased *Smurf2* expression in transgenic endocardium is shown by *in situ* hybridisation at E9.5 (black arrowheads). **F)** Graph of the log fold change (LogFC, RNA-seq) showing the upregulation of *Smurf1* and *Smurf2*. **G)** Representative enriched pathways associated to the top upregulated interactors (Bmp2 interactors with the highest number of direct connections to other DEG). Scale bars, 100 μm.

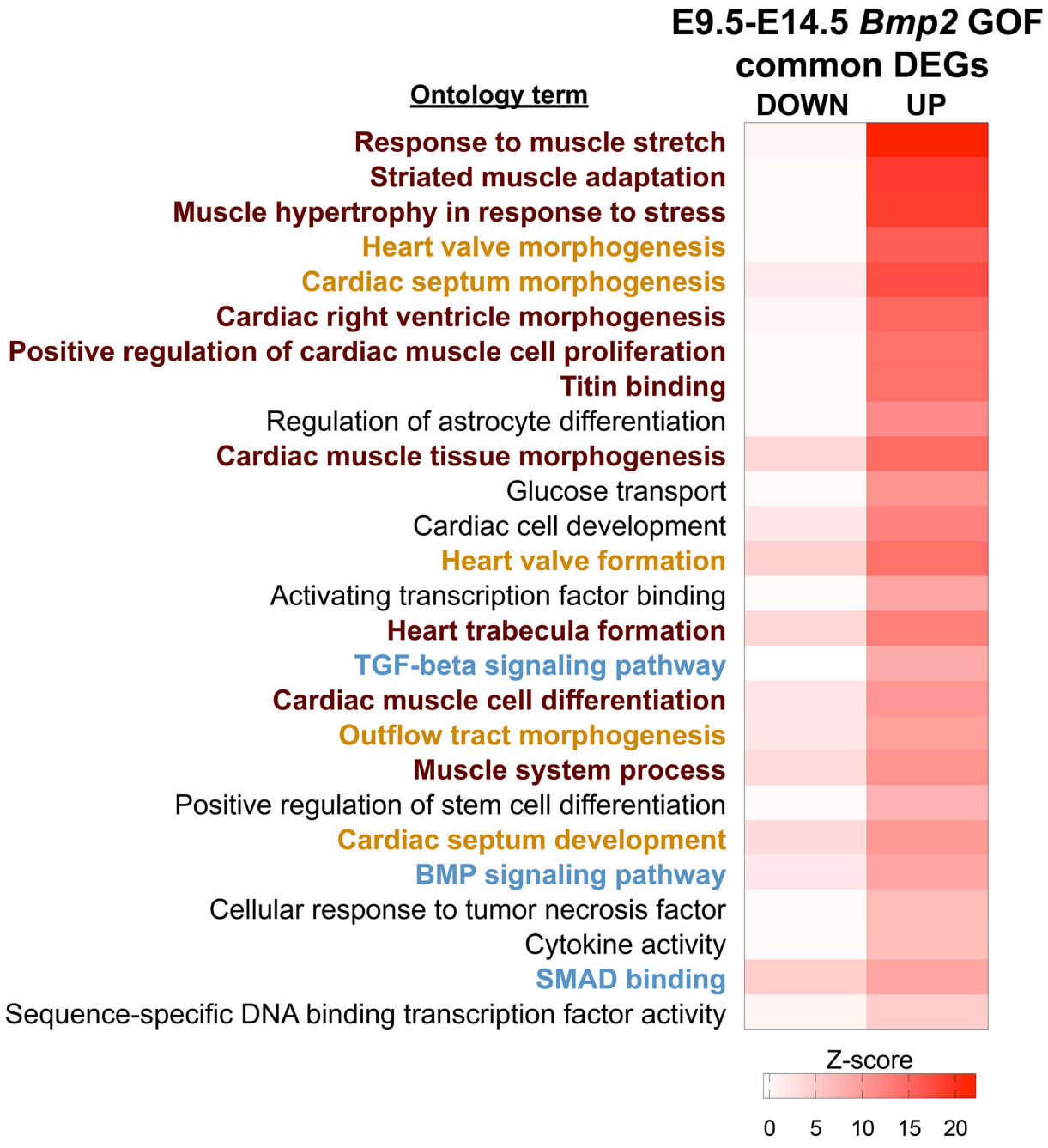

Ankrd1 / Bmp2 / Cx3cl1 / Cyr61 / Edn1 / Ednrb / Egln1 / Fabp5 / Fhl2 / Gata4 / Gata6 / Hey2 / Id2 / Id3 / Igf1 / Mycn / Slc2a1 / Smad6 / Smad7 / Smad9 / Tbx20 / Tbx3 / Tcap / Tnni2 / Trim63 / Vcam1

Fig. S3: Comparison of DEG in two different models of Bmp2 myocardial GOF. Heat map showing the most representative enriched GO and KEGG Pathway terms associated to upregulated DEGs in *Bmp2* GOF hearts at E9.5 (this report) and E14.5 (Prados et al., 2018). The Z-score of each term in common down- or upregulated DEGs is represented in the heat map with different degrees of red. Terms associated with myocardium, valve formation and Bmp pathway are colored in dark red, orange and blue, respectively. Common upregulated DEGs associated to the terms are shown below.

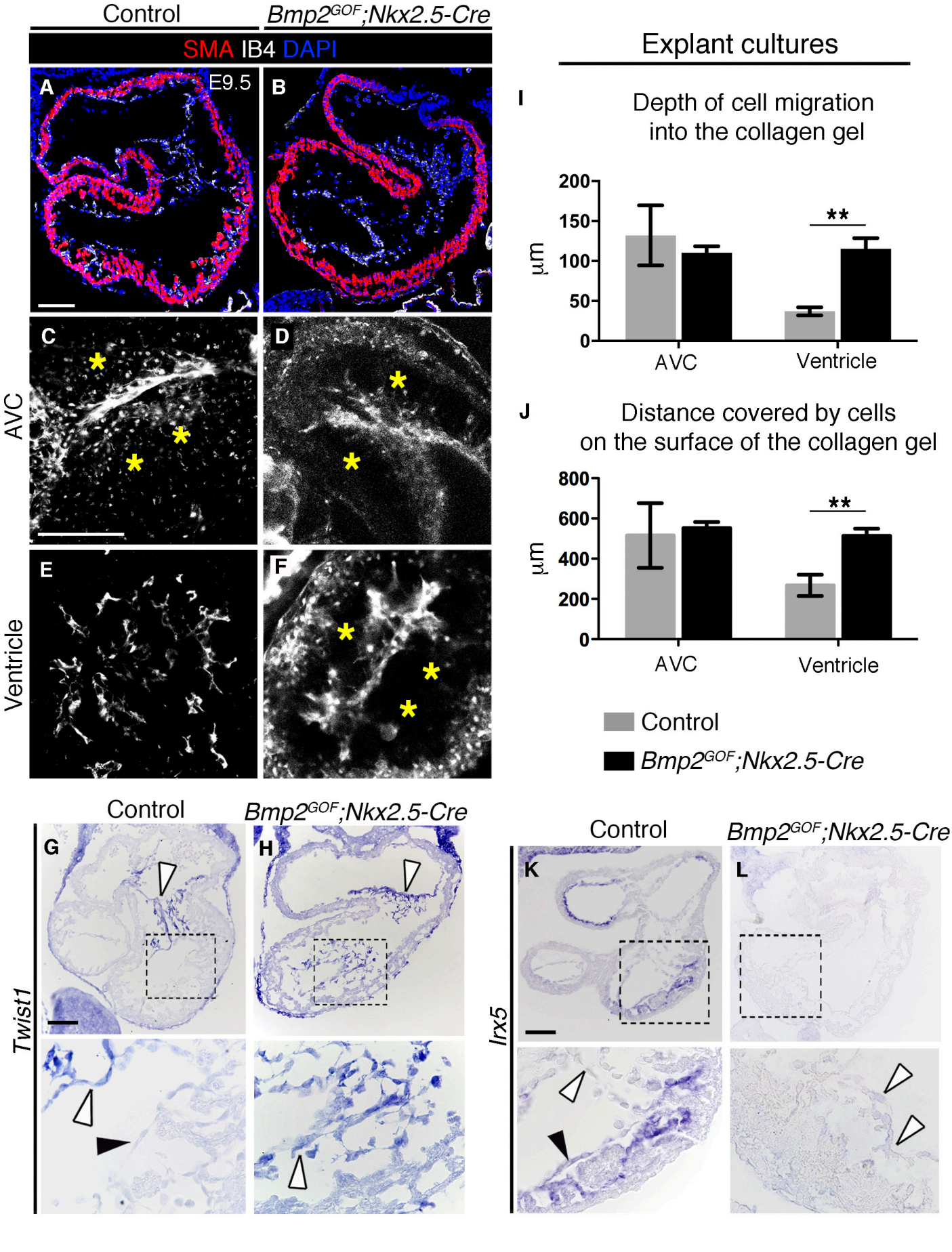

Fig. S4. Expansion of EMT in *Bmp2^{GOF};Nkx2.5-Cre* hearts

A,B) SMA and Isolectin-B4 (IB4) immunostaining of E9.5 control and *Bmp2^{GOF};Nkx2.5-Cre* hearts, marking the myocardium and endocardium (and endocardium-derived cells), respectively. **C-F)** Maximum intensity projections of confocal z-stacks of IB4-immunostained hearts, showing altered endocardial morphology of *Bmp2^{GOF};Nkx2.5-Cre* hearts at E9.5. The ventricular endocardial layer normally envelops the forming trabeculae (E), but in *Bmp2^{GOF};Nkx2.5-Cre* hearts the endocardium accumulates in the center of the lumen (F). **G)** *Twist1* is normally restricted to the AVC. The white arrowhead shows positive AVC endocardium and the black arrowhead the negative ventricular endocardium (inset). **H)** *Twist1* is expanded into the endocardium of transgenic ventricles (white arrowhead inset). **I)** Graph showing the depth of cell invasion of control and transgenic AVC and ventricular explants. **J)** Graph showing the distance covered by control and transgenic AVC and ventricular endocardial cells on the surface of the collagen gel. **K)** In control hearts, *Irx5* is specifically expressed in chamber endocardium (black arrowhead), but is absent from the AVC endocardium (white arrowhead). **L)** Chamber expression of *Irx5* was lost in transgenic hearts (white arrowheads). Scale bars, 100μm. Asterisks (*) indicate statistically significant differences, as assessed by student´s t-test. ** <0.01.

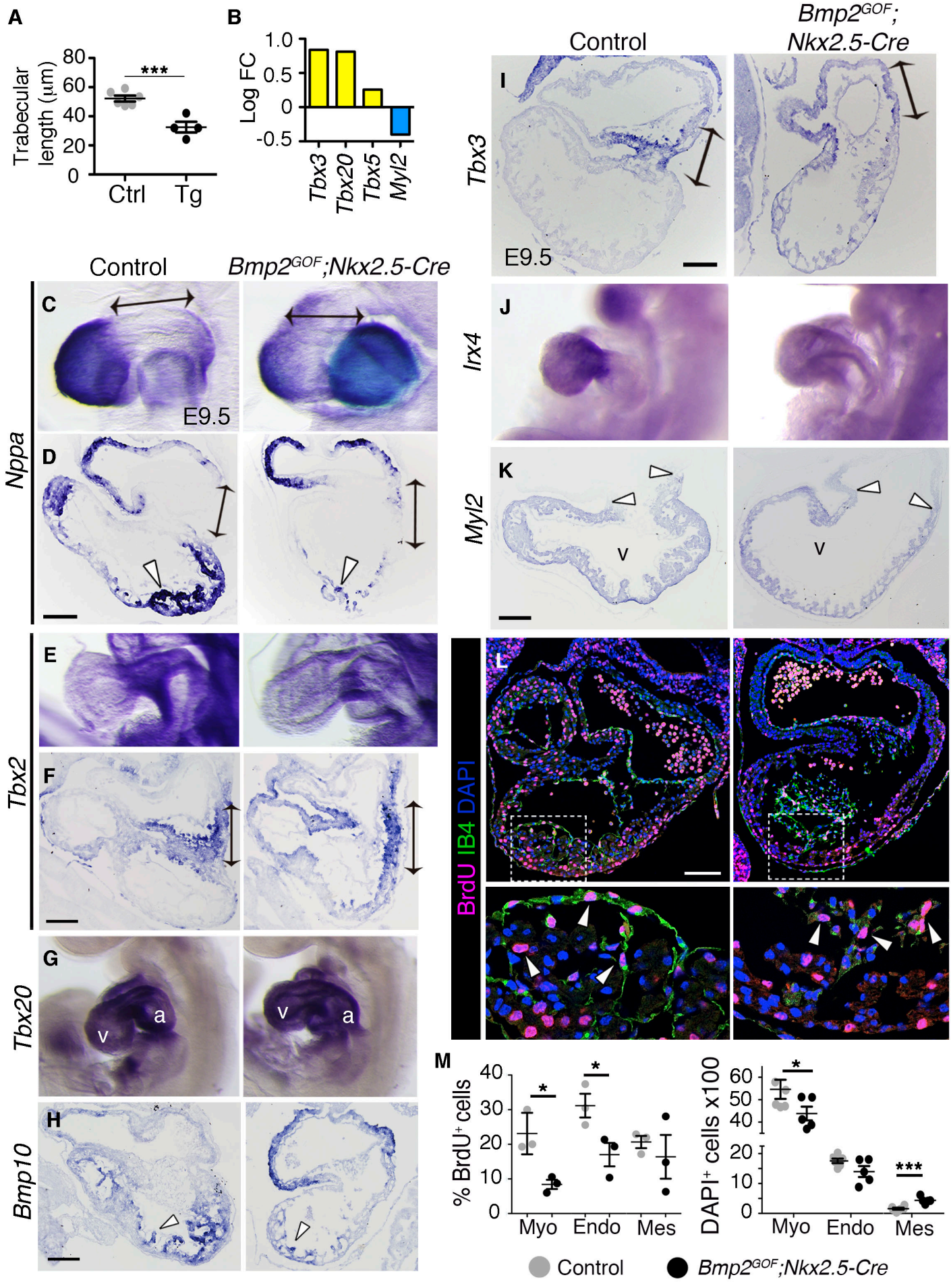

Fig. S5: Unaffected myocardial identity in *Bmp2^{GOF};Nkx2.5-Cre* embryos

A) Ventricular measurements of histological sections. The length of the trabeculae (μm) is significantly reduced in *Bmp2^{GOF};Nkx2.5-Cre* hearts. **B)** Graph of the log fold change (LogFC, RNA-seq) of myocardial-related genes. Yellow graphs show upregulation and blue graphs downregulation. *Tbx2*, *Nppa*, *Bmp10*, and *Irx4* expression levels were not altered. **C,D)** Unaltered expression of *Nppa*, with expression in atrial and ventricular myocardium but not in the AVC (double arrows), shown by wholemount *in situ* hybridisation. **E,F)** *Tbx2 in situ* hybridization showing restricted expression in the AVC in control and *Bmp2^{GOF};Nkx2.5-Cre* hearts. **G)** Expression of *Tbx20* throughout the heart in control and transgenic hearts. **H)** Normal expression of *Bmp10* in the small trabeculae of *Bmp2^{GOF};Nkx2.5-Cre* hearts (arrowheads). **I)** Restriction of *Tbx3* expression to AVC myocardium in control and *Bmp2^{GOF};Nkx2.5-Cre* hearts (double arrows). **J)** Normal expression of *Irx4* in ventricular myocardium of *Bmp2^{GOF};Nkx2.5-Cre* hearts. **K)** Normal expression of the ventricular myocardial marker *Myl2 (Mlc2v)* in transgenic hearts. White arrowheads mark the limit of *Myl2* expression, at the ventricle-AVC border. **L)** Staining with an anti-BrdU antibody (2h pulse, magenta), showing decreased proliferation of myocardial and endocardial cells in *Bmp2^{GOF};Nkx2.5-Cre* hearts. Endocardium and endocardial-derived cells were identified by Isolectin-B4 staining (IB4, green). **M)** Ratio of BrdU-positive cells to the total number of DAPI-positive (DAPI+) cells. DAPI^{+} nuclei as an index of cell number, showing decrease in the number of myocardial cells. V, ventricle; a atrium; myo, myocardial cells; endo, endocardial cells; mes, mesenchymal cells. Scale bars, 100μm. Asterisks (*) indicate statistical significance, as assessed with the student´s t-test. *<0.05; *** <0.001.

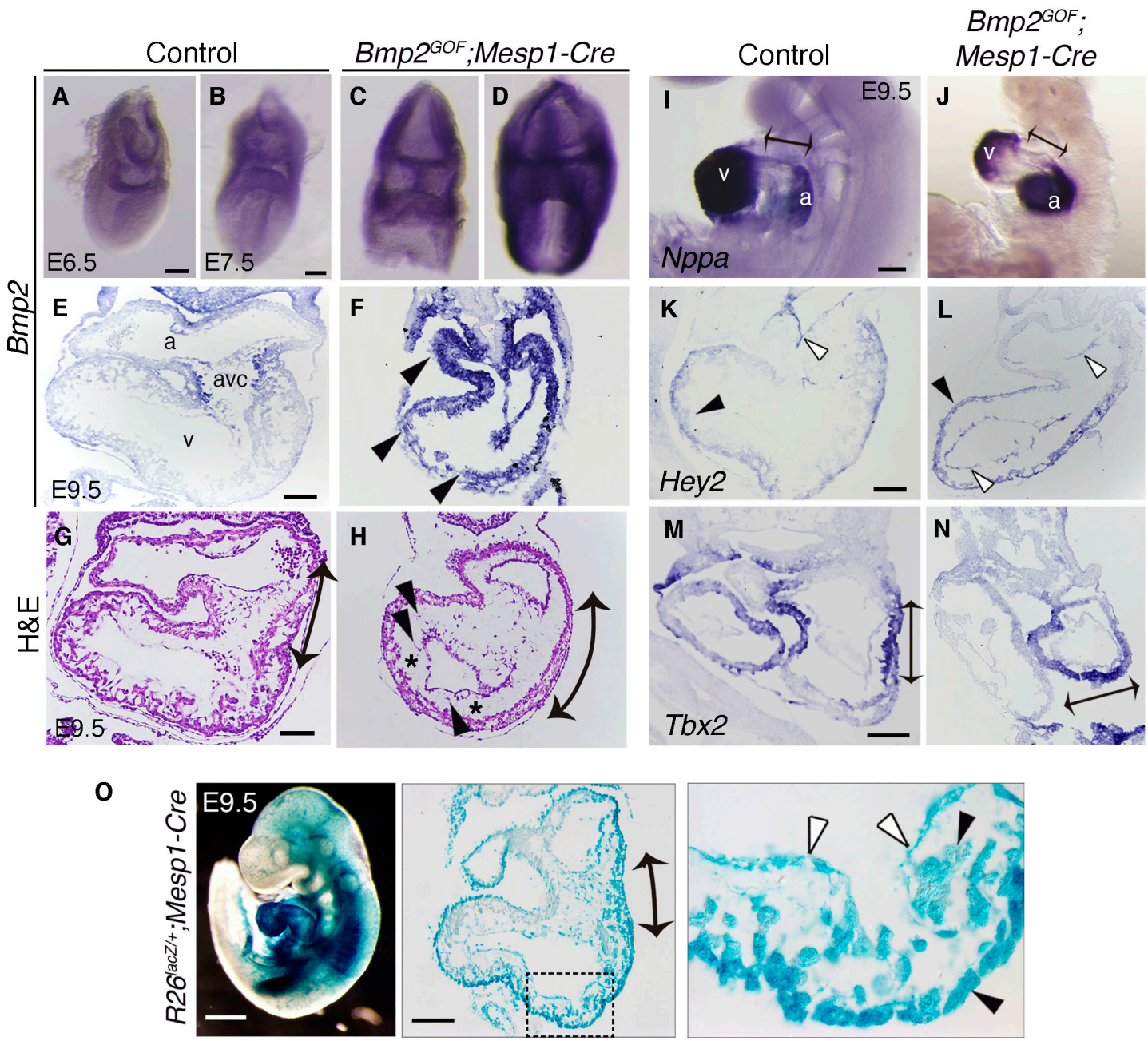

Fig. S6: Unaffected myocardial identity in *Bmp2^{GOF};Mesp1-Cre* embryos

A-D) *Bmp2 in situ* hybridization, showing moderate activation of the transgene in *Bmp2^{GOF};Mesp1-Cre* embryos at E6.5 (A,C) and more pronounced activation at E7.5 (B,D). **E,F)** *Bmp2 in situ* hybridization, showing pronounced activation of the transgene throughout the heart at E9.5 (arrowheads) in *Bmp2^{GOF};Mesp1-Cre* embryos. **G,H)** H&E staining showing severe cardiac defects in *Bmp2^{GOF};Mesp1-Cre* embryos at E9.5. Arrowheads point to ectopic mesenchymal cells within the ventricle. Asterisks show the increased space between endocardium and myocardium. **I,J)** Normal *Nppa* patterning in *Bmp2^{GOF};Mesp1-Cre* embryos. **K,L)** *Hey2 in situ* hybridization showing normal myocardial expression (black arrowheads) and expansion into the endocardium of the ventricle (white arrowheads) in *Bmp2^{GOF};Mesp1-Cre* hearts. **M,N)** *Tbx2 in situ* hybridization, showing restricted expression in the AVC in control and *Bmp2^{GOF};Mesp1-Cre* hearts. **O)** Mesp1-Cre activates β-gal throughout the mesoderm, including the heart in *R26^{lacZ};Mesp1-Cre* embryos. Double arrows delimitate the AVC. White arrowheads point to ventricular endocardium and black arrowheads to ventricular myocardium. v, ventricle; a, atrium. Scale bars, 500μm (O, wholemount), 100μm (all the rest).

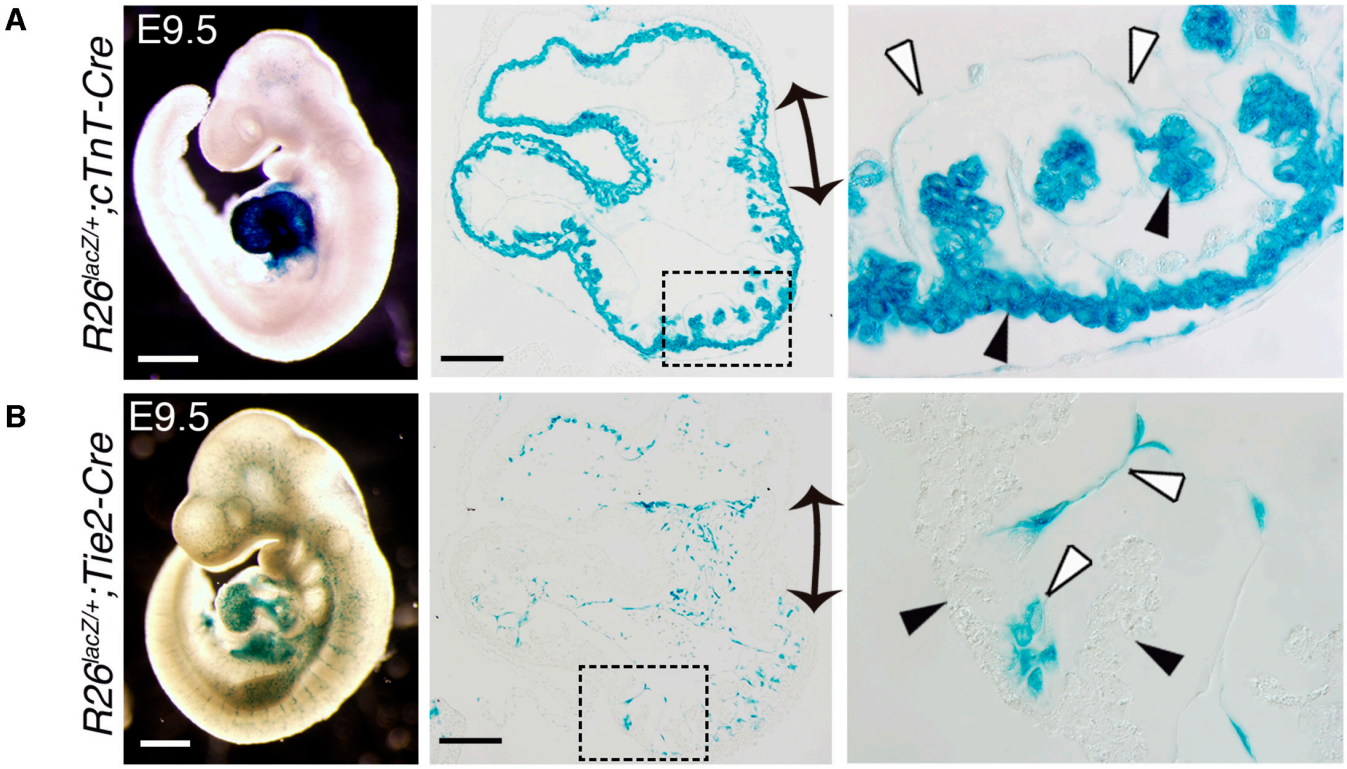

Fig. S7: X-gal staining of *R26^{lacZ};cTnT-Cre* and *R26^{lacZ};Tie2-Cre* lines

X-gal staining, indicating cre-mediated activation of β-galactosidase (β-gal) activity in double heterozygote embryos (*R26^{lacZ};cTnT-Cre* and *R26^{lacZ};Tie2-Cre*), is shown in wholemount and on paraffin sections. **A)** Cardiac TnT-Cre mediates induction of β-gal activity in the myocardium. **B)** Tie2-Cre is active throughout the endothelium, including the endocardium. Double arrows delimitate the AVC. Black arrowheads point to ventricular myocardium and white arrowheads to ventricular endocardium. Scale bars, 500µm (wholemount), 100 µm (sections).

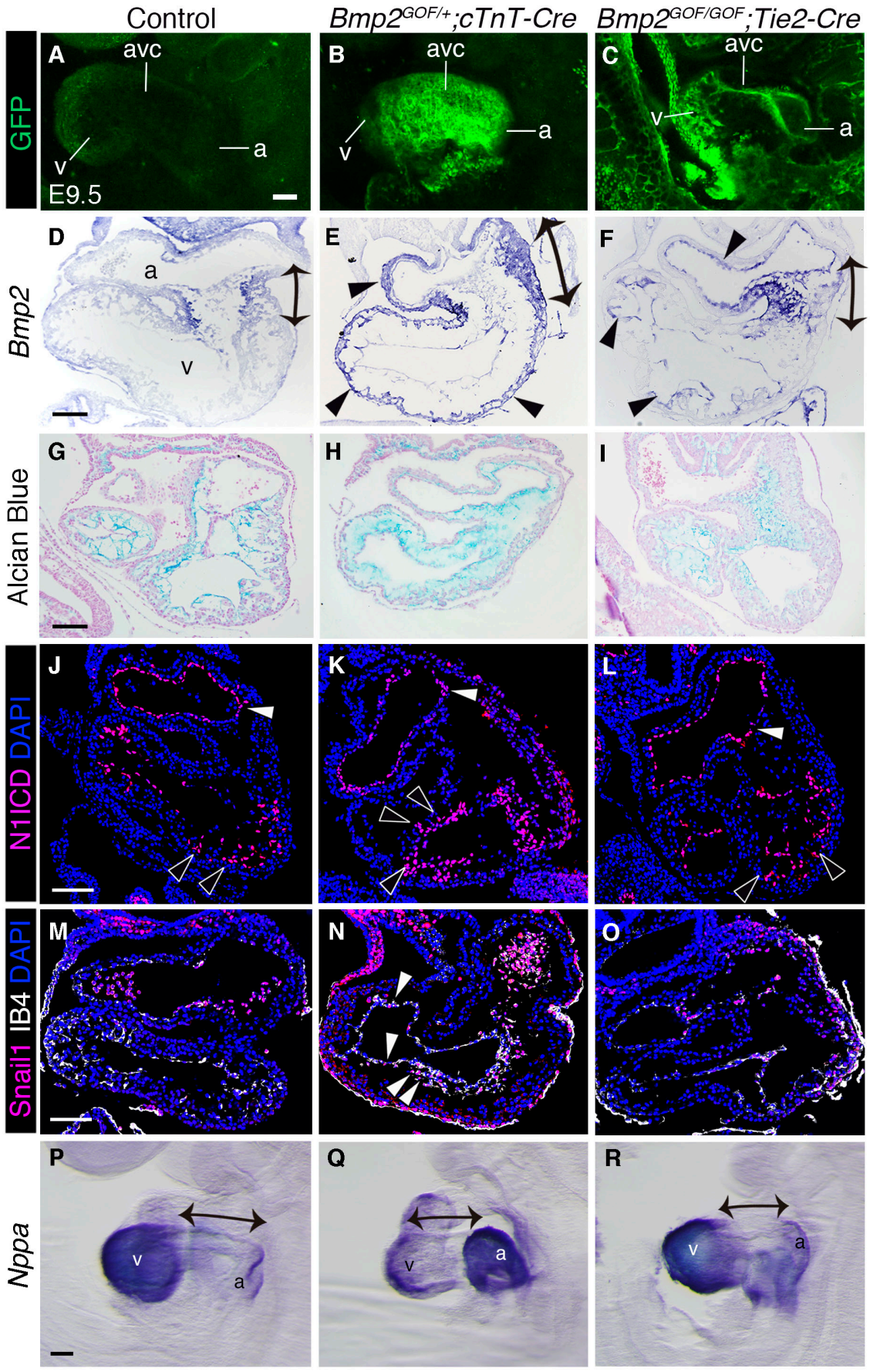

Fig. S8: Ventricular expansion of valve endocardium identity is driven by ectopic myocardial *Bmp2* expression

A) GFP-negative control hearts, (**B**) GFP expressed in the myocardium after *cTnT-Cre*-driven Bmp2-eGFP activation. **(C)** GFP expressed in the endothelium/endocardium after *Tie2-Cre* activation. **D)** *In situ* hybridization showing *Bmp2* expression restricted to AVC myocardium in control E9.5 heart (double arrow delimitates the AVC). Expression was expanded to the corresponding tissue after activation of *cTnT-Cre* **(E,** myocardium, arrowheads**)** and *Tie2-Cre* **(F**, endocardium, arrowheads**)**. Alcian blue staining showing excessive accumulation of ECM in $Bmp2^{GOF}$*;cTnT-Cre* hearts **(H)**, compared to normal, restricted ECM observed in control **(G)** and $Bmp2^{GOF}$*;Tie2-Cre* hearts **(I). J-L)** N1ICD immunostaining (magenta) showing that Notch1 pathway activation occurs throughout the AVC endocardium (white arrowheads) and at the base of the forming trabeculae (black arrowheads) in ventricular endocardium in control hearts **(J)** and $Bmp2^{GOF}$*;Tie2-Cre* hearts **(L)**. The endocardial N1ICD-positive domain expands throughout the ventricle in *cTnT-Cre* hearts **(K)**. **M-O)** Snail1 (magenta), normally restricted to the AVC **(M,O)**, is expanded into the ventricle in $Bmp2^{GOF}$*;cTnT-Cre* hearts **(N)**. The endocardium is counterstained with IB4 (white) and nuclei with DAPI (blue). **P-R)** *Nppa* staining shows unaffected myocardial patterning in $Bmp2^{GOF}$*;cTnT-Cre* **(Q)** and $Bmp2^{GOF}$*;Tie2-Cre* **(R)** hearts. a, atrium; v, ventricle. Scale bars, 100μm.

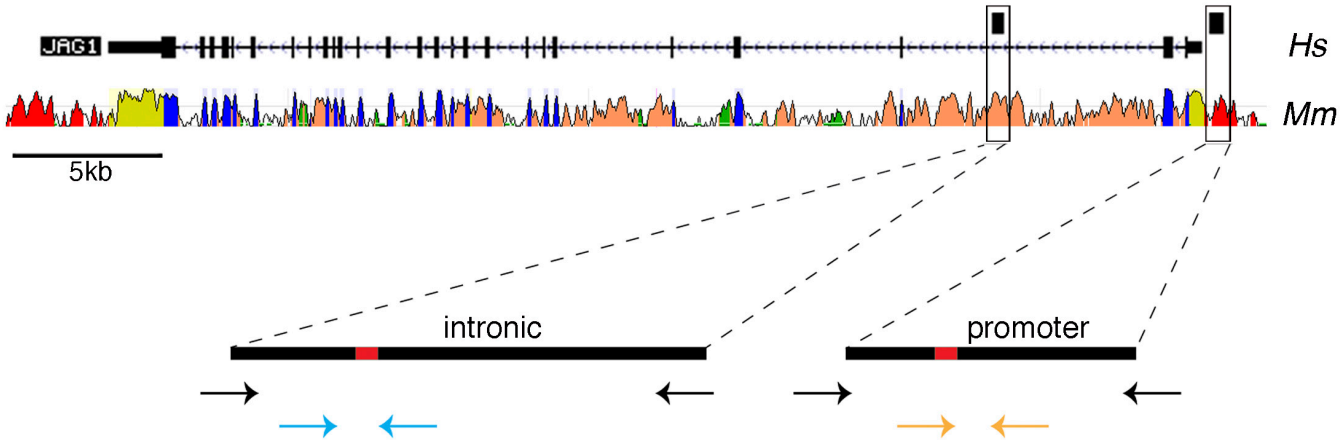

Fig. S9: Smad1 binding sites in the promoter and second intron of *Jag1*

Schematic showing the *JAG1* locus in humans (*Homo sapiens*, *Hs*). Two Smad1 binding sites, shown by Smad1 Chip-seq in HUVEC (Morikawa et al., 2011), are highlighted on the top and magnified on the bottom. The mouse (*Mus musculus*, *Mm*) orthologue *Jag1* and its sequence comparison is shown below the human gene. In the magnified intronic and promoter regions black arrows indicate primers used for the isolation of the regions of interest for the luciferase assays and blue or yellow arrows indicate primers used for qPCR analysis of the Smad1 ChIP data. The red rectangles represent Smad binding consensus sequences.

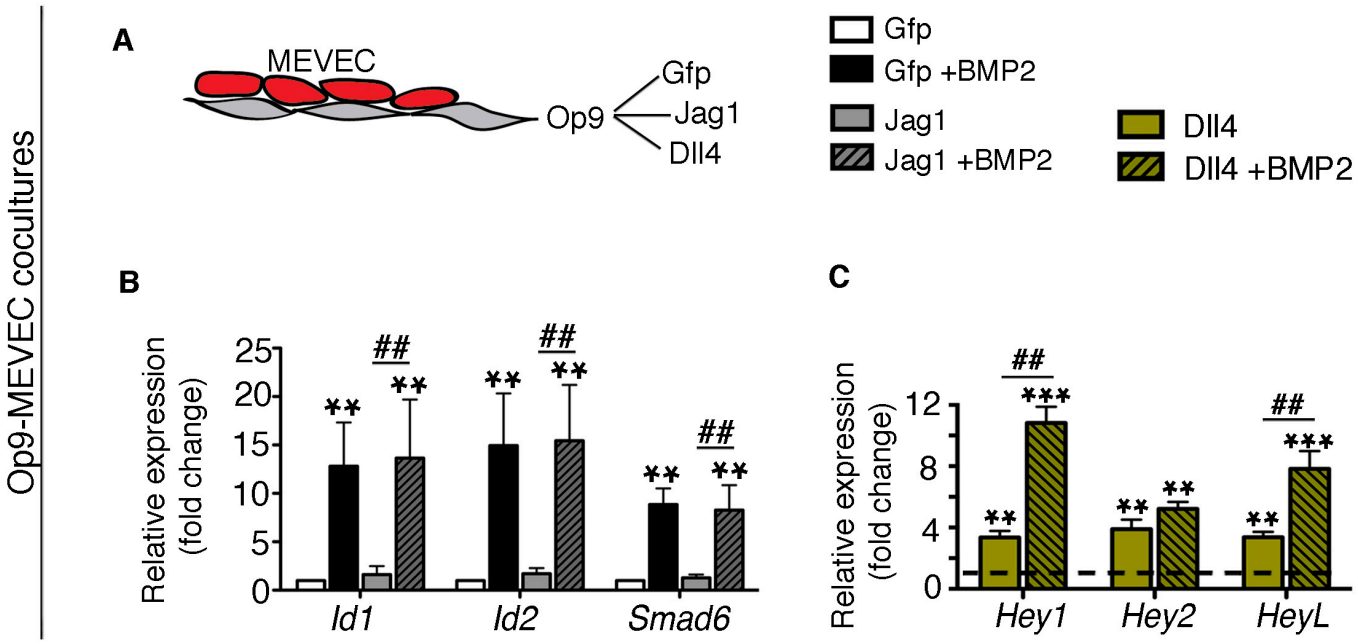

Fig. S10: Bmp and Notch co-operation *in vitro* (MEVEC)

A) Schematic showing the co-culture protocol of MEVEC on OP9 cells, expressing Gfp (control), Jag1 or Dll4. **B)** Bmp target (*Id1*, *Id2*, *Smad6*) gene expression analysis in MEVEC co-cultured with OP9 cells expressing GFP or Jag1 in the presence or absence of human recombinant BMP2. **C)** Notch target (*Hey1, Hey2, HeyL*) gene expression analysis in MEVEC co-cultured with Dll4-expressing OP9 in the presence or absence of BMP2. The dashed line indicates the expression levels in MEVEC co-cultured with GFP-expressing OP9 cells. Asterisks (*) indicate statistical significance compared to the equivalent Gfp control and hashtags (#) indicate differences as shown in the graphs, assessed with the student´s t-test. *<0.05; ** ,##<0.01; *** <0.001.

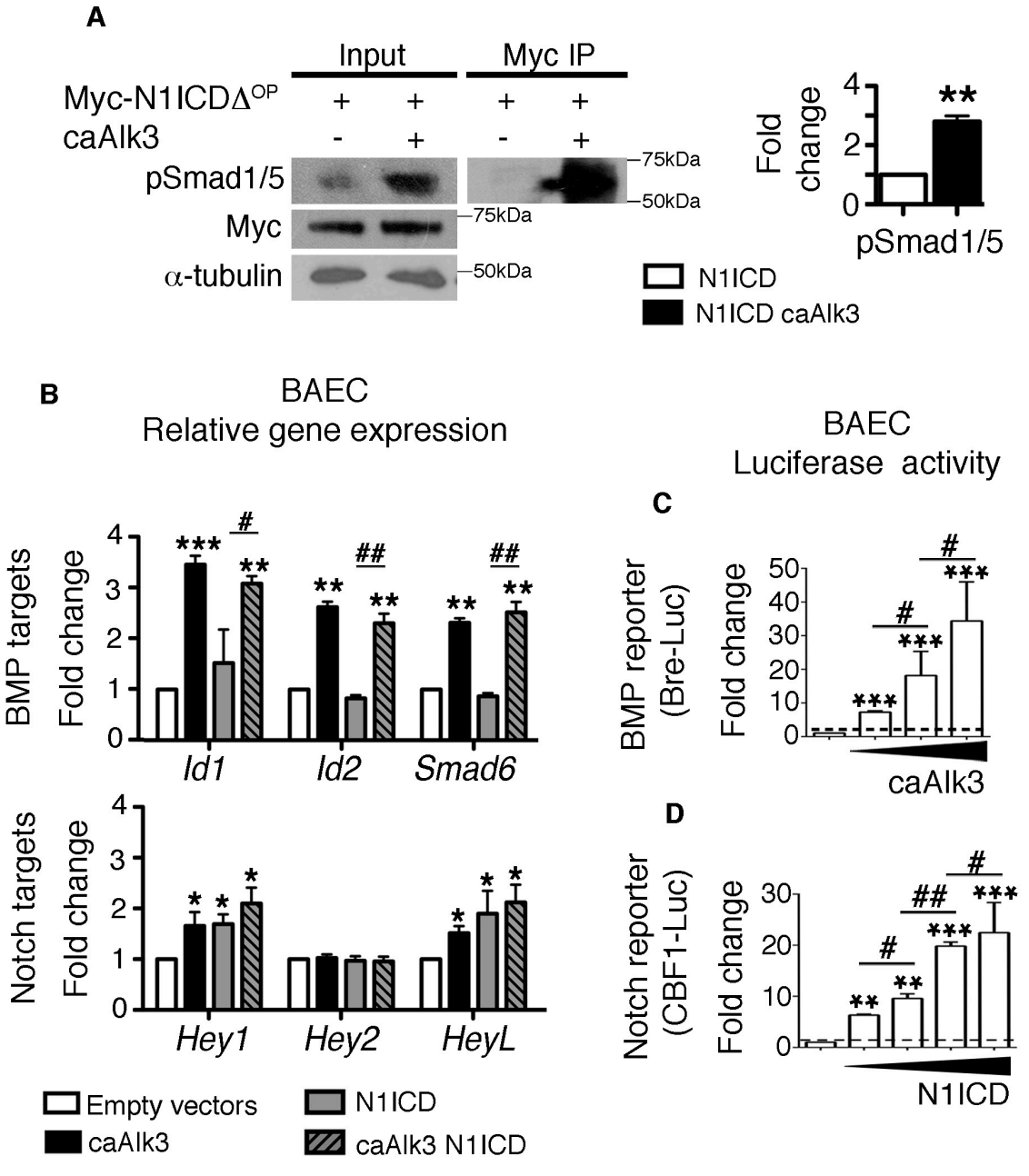

Fig. S11: Bmp and Notch co-operation *in vitro* (BAEC)

A) WB analysis of input and Myc IP with anti-pSmad1/5, anti-Myc and anti-α-tubulin antibodies in BAEC transfected with Myc-tagged N1ICD (Myc-N1ICDΔ^{OP}; this shorter version of N1ICD weights around 70KDa and not the usual 110 KDa) in the presence or absence of caAlk3. Quantification of the input WB (normalised ratios of pSmad1/5 to α-tubulin) is shown in the graph. **B)** Bmp target (*Id1, Id2, Smad6*) and Notch target (*Hey1, Hey2, HeyL*) gene expression analysis in BAEC cultures. Cells were transfected with empty vectors, caAlk3, N1ICD or caAlk3 and N1ICD. **C,D)** Luciferase assays in BAEC with the BRE-Luc (Bmp) and the CBF1-Luc (Notch) reporters. **C)** Transfection with increasing amounts of caAlk3 (25, 50 and 75ng) activates the BRE-Luc reporter in a dose-dependent manner. **D)** Transfection with increasing amounts of N1ICD-expressing plasmid (5, 10, 20 and 40ng) increases CBF1-Luc reporter activity in a dose-dependent manner. Dashed lines indicate the minimal activation of each reporter due to transfection of empty vectors and the Renilla internal control (endogenous). Asterisks (*) indicate statistically significant differences compared with empty vectors; hashtags (#) indicate differences as shown in the graphs. *,# <0.05; **,## <0.01; ***<0.001.

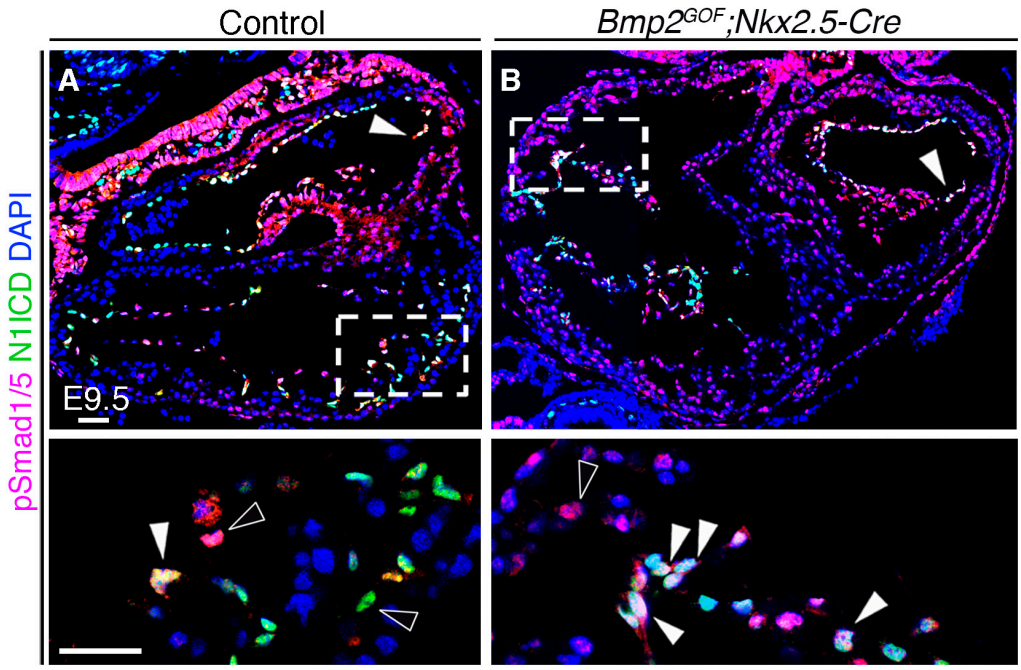

Fig. S12: Bmp and Notch co-localization *in vivo*

A) In E9.5 control hearts, pSmad1/5 (magenta) and N1ICD (green) colocalize in nuclei throughout the AVC endocardium (**A**, white arrowhead) and in a subset of ventricular endocardial cells (white arrowhead in inset). Ventricles also contain isolated cells positive for either N1ICD or pSmad1/5 (black arrowheads). **B)** More extensive pSmad1/5 and N1ICD co-localization in the ventricle of *Bmp2^{GOF};Nkx2.5-Cre* hearts (white arrowheads in inset). Scale bars, 50μm.

Table S1: Viability of genotypes with tissue-specific Bmp2 GOF.

A

	Number of embryos	*Bmp2*$^{GOF/+}$*;Nkx2.5-Cre;*	Controls (*Bmp2*$^{GOF/+}$)
E9.5	136	74 (54.41%)	62 (45.59%)
E10.5	28	8 (28,57%) 7 necrotic (25%)	13 (46.43%)
E11.5	20	1 (5%) 12 necrotic (60%)	7 (35%)

For the *Nkx2.5-Cre* crosses we bred:
Nkx2.5-$^{Cre/Cre}$ females with *Bmp2*$^{GOF/+}$ males (54% of the crosses)
Bmp2$^{GOF/+}$ females with *Nkx2.5-*$^{Cre/Cre}$ males (46% of the crosses)

B

	Number of embryos	*Bmp2* $^{GOF/+}$*;Mesp1-Cre;*	Controls (*Bmp2* $^{GOF/+}$)
E6.5	66	27 (40.91%)	39 (59.09%)
E7.5	59	26 (44.07%)	33 (55.93%)
E9.5	96	49 (51.04%) 6 necrotic (6.25%)	41 (42.71%)
E10.5	48	4 (8.33%) 22 necrotic (45.83%)	22 (45.83%)

For the *Mesp1-Cre* crosses we bred *Bmp2*$^{GOF/GOF}$ females and *Mesp1*$^{-Cre/+}$ males.

C

	Number of embryos	*Bmp2* $^{GOF/+}$*;cTnT-Cre;*	Controls (*Bmp2* $^{GOF/+}$)
E9.5	62	35 (56.45%)	27 (43.55%)
E10.5	30	9 (30%) 4 necrotic (13.33)	17 (56.66%)

For the *cTnT-Cre* crosses we bred *Bmp2*$^{GOF/GOF}$ females with *cTnT-Cre* heterozygote males.

D

	Number of embryos	*Bmp2* $^{GOF/GOF}$*;Tie2-Cre*	Controls (all other genotypes)
E9.5	32	7 (21.88%)	25 (78.12%)
E10.5	21	4 (19%)	17 (81%)
E11.5	30	10 (33.33%)	20 (66.66%)
E14.5	15	4 (26.67%)	11 (73.33%)
E17.5	20	2 (10%) 6 necrotic (30%)	12 (60%)

For the *Tie2-Cre* crosses we bred:
Bmp2$^{GOF/GOF}$ females with *Bmp2*$^{GOF/+}$;*Tie2*$^{-Cre/+}$ males (44% of the crosses)
Bmp2$^{GOF/+}$; *Tie2*$^{-Cre/+}$ females with *Bmp2*$^{GOF/GOF}$ males (56% of the crosses)

Table S2: RNA-seq analysis of E9.5 Bmp2 GOF hearts

Sheet 1: List of differentially expressed genes (DEG) in RNA-seq. DEG identified by RNA-seq (P<0.005) in E9.5 *Bmp2*^{GOF}*;Nkx2.5-Cre* hearts. 2,646 genes were upregulated (yellow) and 2,538 were downregulated (blue).

Sheet 2: Gene ontology (GO) analysis of RNA-seq. Overrepresentation analysis of GO terms and KEGG pathways for upregulated and downregulated genes (P<0.005).

Sheet 3: Overlapping GO analysis of RNA-seq. Z-score values for different GO terms and KEGG pathways in each subgroup of Sheet 2.

Sheet 4: STRING_input

Sheet 5: STRING_output

Sheet 6: GO analysis network. Overrepresentation analysis of GO terms and KEGG pathways for DEG functionally related to BMP2 on a first-second degree or on a third-fifth degree.

Sheet 7: Overlapping GO analysis of network. Z-score values for different GO terms and KEGG pathways in each subgroup of Sheet 4.

Sheet 8: Pathway analysis of hubs. Overrepresentation analysis of KEGG Pathways for the selected nodes and their direct interactors.

* Data are the standard output from GO Elite.

Click here to Download Table S2

Table S3. Excel file showing the comparison of the DEG in E11.5 Bmp4 OE mandibles and E9.5 Bmp2 GOF hearts.

Click here to Download Table S3

Table S4. Excel file showing the comparison of the DEG in E9.5 Bmp2 GOF hearts and E14.5 Bmp2 GOF hearts.

Click here to Download Table S4

Supplementary Movies

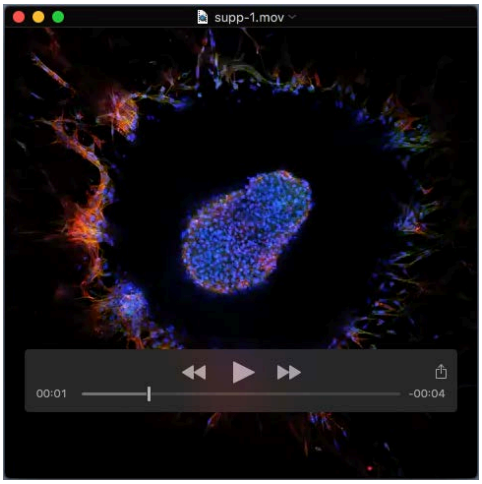

Movie S1: Control AVC explant

Control AVC explant cultured on collagen gel. The explant was immunostained with a mesenchymal marker (α-smooth muscle actin, SMA, magenta) and an actin cytoskeletal marker (phalloidin, green). Endocardial-derived mesenchymal cells (magenta) have migrated away from the center of the explant and invaded the collagen matrix.

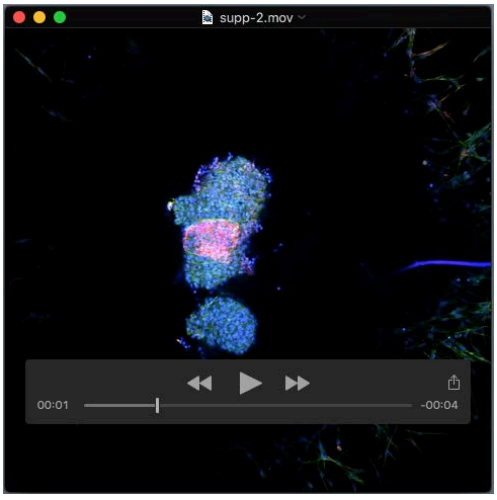

Movie S2: *Bmp2^{GOF};Nkx2.5-Cre* AVC explant

Bmp2^{GOF};Nkx2.5-Cre AVC explant cultured on collagen gel. Immunostaining as previously described. Endocardial-derived mesenchymal cells (magenta) have migrated away from the center of the explant and invaded the collagen matrix.

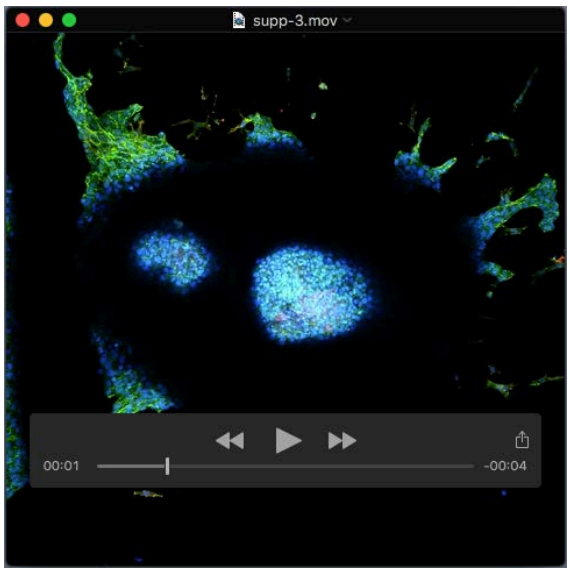

Movie S3: Control ventricular explant

Control ventricular explant cultured on collagen gel. Immunostaining as previously described. Ventricular endocardium is not able to transform and migrate. It thus forms a compact monolayer on the surface of the collagen matrix.

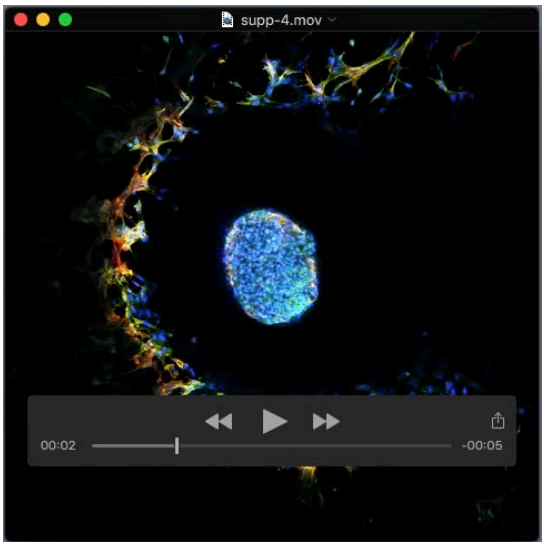

Movie S4: *Bmp2^{GOF};Nkx2.5-Cre* ventricular explant

Bmp2^{GOF};Nkx2.5-Cre ventricular explant cultured on collagen gel. Immunostaining as previously described. The transgenic ventricular tissue behaves like AVC tissue and is able to migrate, transform and invade the collagen gel.

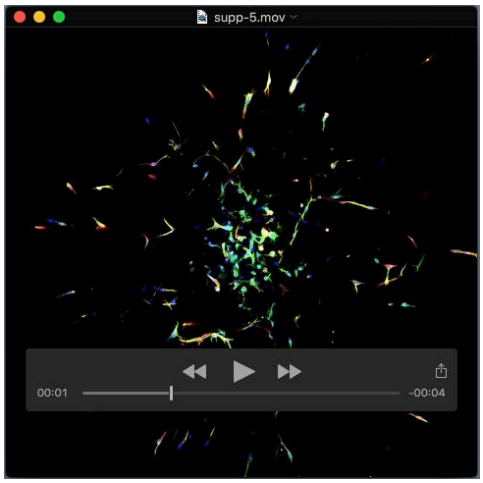

Movie S5: *Bmp2^{GOF};Nkx2.5-Cre* ventricular explant treated with DMSO (vehicle)

Bmp2^{GOF};Nkx2.5-Cre ventricular explant cultured on collagen gel with DMSO. Immunostaining as previously described. The explant behaves like a wild-type AVC explant.

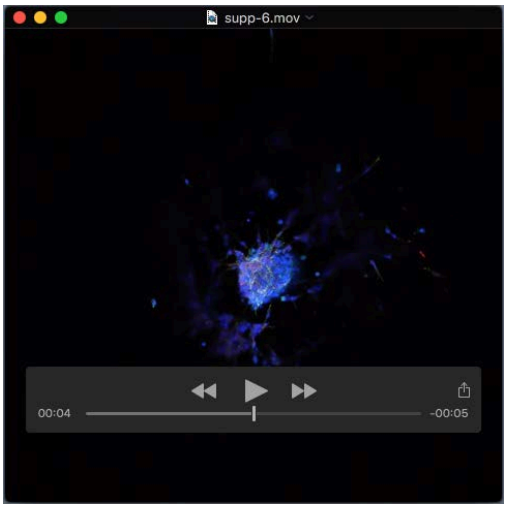

Movie S6: *Bmp2^{GOF};Nkx2.5-Cre* ventricular explant treated with RO4929097 (RO, Notch inhibitor)

Bmp2^{GOF};Nkx2.5-Cre ventricular explant cultured on collagen gel with RO. Immunostaining as previously described. 3D invasion is severely suppressed.pr

References

Morikawa, M., Koinuma, D., Tsutsumi, S., Vasilaki, E., Kanki, Y., Heldin, C. H., Aburatani, H. and Miyazono, K. (2011). ChIP-seq reveals cell type-specific binding patterns of BMP-specific Smads and a novel binding motif. *Nucleic acids research* **39**, 8712-8727.

Prados, B., Gomez-Apinaniz, P., Papoutsi, T., Luxan, G., Zaffran, S., Perez-Pomares, J. M. and de la Pompa, J. L. (2018). Myocardial Bmp2 gain causes ectopic EMT and promotes cardiomyocyte proliferation and immaturity. *Cell Death Dis* **9**, 399.